Construction of explicitly correlated geminal-projected particle-hole creation operators for many-electron systems using the diagrammatic factorization approach

Michael G. Bayne, Yuki Uchida, Joshua Eller, Carena Daniels, and Arindam Chakraborty*
Department of Chemistry, Syracuse University, Syracuse, New York 13244, USA
(Received 13 April 2016; revised manuscript received 19 September 2016; published 3 November 2016)

The computational cost of performing a configuration interaction (CI) calculation for treating electron-electron correlation is directly proportional to the number of terms in the CI expansion. In this work, we present a diagrammatic projection approach for *a priori* identification of noncontributing terms in a CI expansion. This method known as the geminal-projected configuration interaction (GP-CI) method is based on using a two-body R12 geminal operator for describing electron-electron correlation in a reference many-electron wave function. The diagrammatic projection procedure was performed by first deriving the Hugenholtz diagrams of the energy expression of the R12 reference wave function and then performing diagrammatic factorization of effective particle-hole creation operators. The projection operation, which is a functional of the geminal function, was defined and used for the construction of the geminal-projected particle-hole creation operators. The form of the two-body R12 geminal operator was derived analytically by imposing an approximate Kato cusp condition. A linear combination of the geminal-projected one-particle one-hole and two-particle two-hole operators were used for the construction of the GP-CI wave function. The applicability and implementation of the diagrammatic projection method was demonstrated by performing proof-of-concept calculations on an isoelectronic series of 10 electron systems: CH_4, NH_3, H_2O, HF, and Ne. The results from the calculations show that compared to conventional CI calculations, the GP-CI method was able to substantially reduce the size of the CI space (by a factor of 6–9) while maintaining an accuracy of 10^{-5} Hartrees for the ground-state energies. These results demonstrate the ability of the diagrammatic projection procedure to identify noncontributing states using an analytical form of the R12 geminal correlator operator. The geminal-projection method was also applied to second-order Møller-Plesset perturbation theory (GP-MP2) giving similar results to the GP-CI method in terms of reduction of the double excitation space and accuracy to the ground-state energy. This work also extends the analytical derivation of the geminal-projected particle-hole creation operators that were used for the construction of the CI wave function to coupled-cluster theory (GP-CCSD). This general derivation can also be applied to other many-electron theories and multideterminant quantum Monte Carlo calculations.

DOI: 10.1103/PhysRevA.94.052504

I. INTRODUCTION

An accurate description of correlation energy is needed in order to describe a chemical system. In recovering this correlation energy, the method of configuration interaction (CI) [1] is one of the most successful methods due to the simplicity of its underlying mathematics and its variational properties. Also, it is well known that in the limit of infinite basis, full configuration interaction (FCI) will solve the Schrödinger equation exactly, which makes FCI an important benchmark for any method that treats electron correlation.

One of the challenges in performing CI calculations is the rapid increase in the size of the CI space. However, post calculation analysis of the converged CI vector reveals that a large number of configurations in the CI expansion are noncontributing in the sense that if these configurations were removed, the CI energy of the system would remain essentially the same. Therefore, to reduce the size of the CI space and decrease the computation cost of the CI calculation, it is important to identify the contributing configurations before the start of the CI calculation and to select only important configurations in the CI expansion. Extensive research has been done to effectively truncate the CI space to reduce computational time. A method widely used to select only the important configurations is based on many-body perturbation theory [2–10]. In such studies, the configurations are chosen based either on their energy [2,4,10] or their coefficients in the first-order wave function [3,5]. From these criteria, states will either be accepted or rejected based on a given threshold [11–13]. Examples of these approaches include the multi-reference double-excitation CI (MRD-CI) method [4,14] and the CIPSI (configuration interaction perturbing a multiconfigurational zeroth-order wave function selected iteratively) method [3,5,7]. In related work, Roth *et al.* introduced an iterative importance truncation (IT-CI) scheme that aims at reducing the dimensions of the model space of configuration interaction approaches by an *a priori* selection of the physically most relevant basis states. Using an importance measure derived from multiconfigurational perturbation theory in combination with an importance threshold, they constructed a model space optimized for the description of individual eigenstates of a given Hamiltonian [8,9]. Another method to reduce the cost of the CI calculation is with an integral-direct CI approach. The Saebø-Almlöf algorithm is a direct integral transformation method with low memory requirements [15]. Efficient integral screening was shown in the framework of local-correlation methods [16–21] and also for truncation of virtual orbitals [22–24].

*archakra@syr.edu

Determinants can also be selected based on Monte Carlo methods [25–30]. Greer proposed a Monte Carlo CI method (MCCI) [25–27] to estimate the correlation energies. In this method, a configuration is generated by randomly branching to new configurations in the expansion space. Then the configuration is kept or discarded based on its weight in the wave function. This process is repeated until a desired convergence in the variational energy is achieved. Greer's method is an integral direct method in which the matrix elements H_{AB} are calculated directly during each iteration of the matrix diagonalization step. Sambataro *et al.* presented a variational subspace diagonalization method [31] that finds the relevant configurations by means of iterative sequences of diagonalizations of spaces of reduced size. Each diagonalization provides an energy-based importance measure that governs the selection of the configurations to be included in the states. Similar to Greer's method, which uses Monte Carlo, Booth *et al.* and Petruzeilo *et al.* presented a new stochastic method called full configuration interaction quantum Monte Carlo (FCIQMC) [28–30,32,33]. While Greer's method [25–27] is a subspace diagonalization method, the FCIQMC method takes a different approach in that it represents the wave function in terms of a set of discretized "walkers." The walkers carry a positive or negative sign, inhabit Slater determinant space, and evolve according to a set of rules that includes spawning, death, and annihilation processes. This method is capable of converging onto the FCI energy and wave function of the problem without any *a priori* information regarding the nodal structure of the wave function. Bytautas *et al.* found that a good approximation to the FCI expansion can be obtained based on seniority or the number of unpaired electrons in a determinant [34]. For example, if there are no unpaired electrons in a determinant, the seniority will be zero; if there are two unpaired electrons in a determinant, the seniority will be two, and so on. Another interesting technique for reducing the CI space is known as Löwdin partitioning [35–37]. Ten-no also presented a novel quantum Monte Carlo method in configuration space, which stochastically samples the contribution from a large secondary space to the effective Hamiltonian in the energy-dependent partitioning of Löwdin [38]. Earlier studies showed that the slow convergence of the CI expansion with respect to the size of the one-particle basis is related to poor treatment of the electron-electron cusp condition [39]. As a consequence, a better description of electron-electron correlation can be obtained by including explicit electron-electron distance-dependent terms in the form of the many-electron wave function.

There have been very important results from methods such as quantum Monte Carlo [33,40–49], transcorrelated methods [50], and R12 or F12 methods which show that the inclusion of the r_{12} term in the form of the wave function results in a faster convergence of the CI energies. In the variational Monte Carlo (VMC) method, the Jastrow function is used for including the explicit r_{12} terms in the wave function [40,41]. The Jastrow function can also be augmented by a linear combination of determinants [51–65]. In the transcorrelated method, a similarity transformation is performed on the Hamiltonian using an explicitly correlated function [50,66,67]. Explicit dependence on the r_{12} term in the wave function has been implemented in other methods such as MP2-R12, [68–71] and coupled cluster [72–77], and geminal augmented multiconfigurational self-consistent field (MCSCF) [78]. The applicability of a geminal operator approach for treating electron correlation [79–81] has also been demonstrated by Rassolov *et al.* in a series of articles for various chemical systems [82–88]. A congruent-transformed approach using an explicitly correlated geminal operator has also been developed by Elward *et al.* [89] and Bayne *et al.* [90].

The goal of this work is to use an explicitly correlated reference function to project out noncontributing terms in a CI expansion before the start of the CI calculation. Starting with an ansatz for the explicitly correlated wave function and using many-body diagrammatic techniques, we derive effective particle-hole excitation operators that project out low-amplitude excitations. The key difference between the method presented here and other approaches described above is that the present method does not use an energy-based scheme or perturbation-theory-based criteria to eliminate configurations from the CI expansion. The elimination of configurations is solely based on particle-hole excitation amplitudes derived from an underlying explicitly correlated wave function. The derivation of the method and construction of the explicitly correlated wave function are presented in Secs. II A and II B. The method has been applied to many-electron systems, and proof-of-concept calculations of isoelectronic series of second-row molecules are presented in Sec. III.

II. THEORY AND COMPUTATIONAL DETAILS

A. Diagrammatic factorization of particle-hole excitation operators

The derivation relies on the existence of an explicitly correlated wave function for the many-electron system. In this work, we assumed the following general form for the R12 operator:

$$|\Psi_G\rangle = G|\Phi_0\rangle, \tag{1}$$

where G is assumed to be a two-body operator of the following form:

$$G = \sum_{i<j} g(i,j) \equiv \sum_{i<j} g(r_{ij}). \tag{2}$$

In the above expression, the function g depends on the electron-electron separation distance r_{12}. The following derivation does not depend on the specific functional form of g and its discussion is postponed until Sec. II B. The ground-state energy is obtained by performing minimization over function g.

$$E_G = \min_g \frac{\langle 0|G^\dagger H G|0\rangle}{\langle 0|G^\dagger G|0\rangle}. \tag{3}$$

The energy expression can be expressed by performing congruent transformation on the many-electron Hamiltonian.

$$G^\dagger H G = \left[\sum_{i<j} g(i,j)\right]\left[\sum_i h_1(i) + \sum_{i<j} h_2(i,j)\right]\left[\sum_{i<j} g(i,j)\right]. \tag{4}$$

The transformed operator can be expressed as a sum of the two-, three-, four-, five-, and six-body operators as shown in

the following equation:

$$G^\dagger HG = \sum_{i_1<i_2} w_2(i_1,i_2) + \sum_{i_1<i_2<i_3} w_3(i_1,i_2,i_3) + \sum_{i_1<i_2<i_3<i_4} w_4(i_1,i_2,i_3,i_4) + \sum_{i_1<i_2<i_3<i_4<i_5} w_5(i_1,i_2,i_3,i_4,i_5) + \sum_{i_1<i_2<i_3<i_4<i_5<i_6} w_6(i_1,i_2,i_3,i_4,i_5,i_6). \quad (5)$$

The expectation value of the congruent-transformed Hamiltonian with respect to the Fermi vacuum state is given by

$$\begin{aligned}
&\langle 0|G^\dagger HG|0\rangle \\
&= \frac{1}{2}\sum_{i_1 i_2}^{N}\langle i_1 i_2|w_2(1,2)|i_1 i_2\rangle_A \\
&\quad + \frac{1}{3!}\sum_{i_1 i_2 i_3}^{N}\langle i_1 i_2 i_3|w_3(1,2,3)|i_1 i_2 i_3\rangle_A \\
&\quad + \frac{1}{4!}\sum_{i_1 i_2 i_3 i_4}^{N}\langle i_1 i_2 i_3 i_4|w_4(1,2,3,4)|i_1 i_2 i_3 i_4\rangle_A \\
&\quad + \frac{1}{5!}\sum_{i_1 i_2 i_3 i_4 i_5}^{N}\langle i_1 i_2 i_3 i_4 i_5|w_5(1,2,3,4,5)|i_1 i_2 i_3 i_4 i_5\rangle_A \\
&\quad + \frac{1}{6!}\sum_{i_1 i_2 i_3 i_4 i_5 i_6}^{N}\langle i_1 i_2 i_3 i_4 i_5 i_6|w_6(1,2,3,4,5,6)|i_1 i_2 i_3 i_4 i_5 i_6\rangle_A.
\end{aligned} \quad (6)$$

In the above expression, we follow the convention that indices i, j, k, l correspond to occupied molecular orbitals, a, b, c, d correspond to unoccupied molecular orbitals, and p, q, r, s refer to general molecular orbitals. As expected, the energy expression depends only on the occupied orbitals.

In the next step, the components of the energy expression are expressed using diagrammatic notation. Generally, diagrammatic analysis in many-electron systems is performed using antisymmetrized Goldstone diagrams. However, in this work we used the much more compact Hugenholtz diagrams to keep the number of diagrams tractable. The diagrammatic representation of the energy terms is given by diagrams labeled as D_1, D_2, D_3, D_4, and D_5 in Fig. 1. The vertex of each diagram represents the corresponding w_k operator in Eq. (6). In the next step, the vertex of each diagram is split into two vertices. This is done by analyzing the action of operator g on the occupied orbitals. Specifically, without loss of any generality, the action of the g on the occupied space is given by

$$g(1,2)|i_1 i_2\rangle = \sum_{p_1 p_2}^{\infty}\langle p_1 p_2|g|i_1 i_2\rangle|p_1 p_2\rangle, \quad (7)$$

where the orbitals p_1 and p_2 span both occupied and unoccupied space and i_1 and i_2 span occupied space. It is important to note that Eq. (7) is not the definition of the g operator because it does not define its action on unoccupied orbitals. The above expansion allows us to split the vertices of each diagram shown in Fig. 1, and the resulting diagrams of this transformation are shown in Fig. 2. Algebraically, this is achieved by partitioning the one-particle space into occupied (denoted by i, j, k, l indices) and unoccupied space (denoted by a, b, c, d indices):

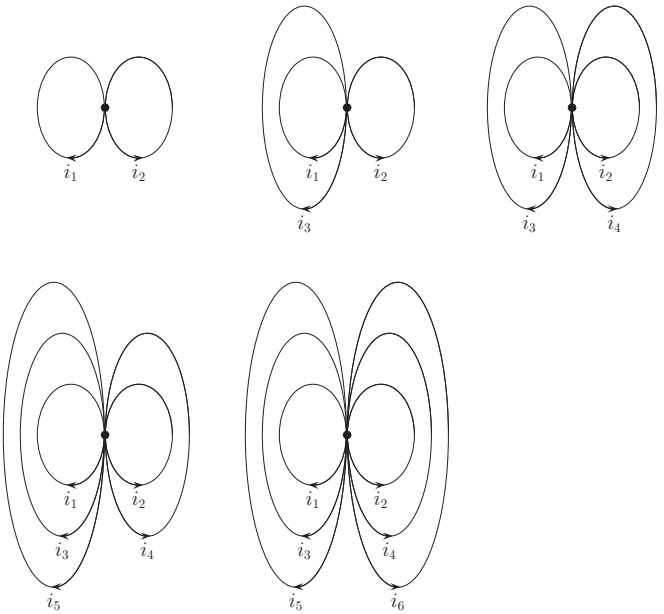

FIG. 1. Diagrams 1–5.

$$\sum_p = \sum_{i=1}^{N} + \sum_{a=N+1}. \quad (8)$$

A detailed description of the algebraic form of the various matrix elements associated with the diagrams are presented in the Appendix. Analysis of the resulting diagrams reveals that a subset of diagrams can be simplified by factoring out common particle-hole (p-h) excitation operators which are shown in Fig. 3. Specifically, diagrams in Fig. 2 can be factorized as 2p-2h (Fig. 4) and 1p-1h operators (Fig. 5). It is important to note that this factorization is performed for all orders of many-particle operators ($w_2, \ldots, w_6$). From Fig. 3, the 2p-2h excitation has the form

$$W_2 = \frac{1}{4}\sum_{i_1 i_2 a_1 a_2} g^{\mathrm{A}}_{i_1 i_2 a_1 a_2}\{a_1^\dagger a_2^\dagger i_2 i_1\}, \quad (9)$$

where

$$g^{\mathrm{A}}_{i_1 i_2 a_1 a_2} = \langle i_1 i_2|g(1,2)(1-P_{12})|a_1 a_2\rangle, \quad (10)$$

and indices i and a represent occupied and unoccupied states, respectively. Similarly, the 1p-1h excitation operator is defined as

$$W_1 = \sum_{i_1 a_1} g_{i_1 a_1}\{a_1^\dagger i_1\}, \quad (11)$$

where

$$g_{i_1 a_1} = \sum_{k_2}^{N} g^{\mathrm{A}}_{i_1 k_2 a_1 k_2}, \quad (12)$$

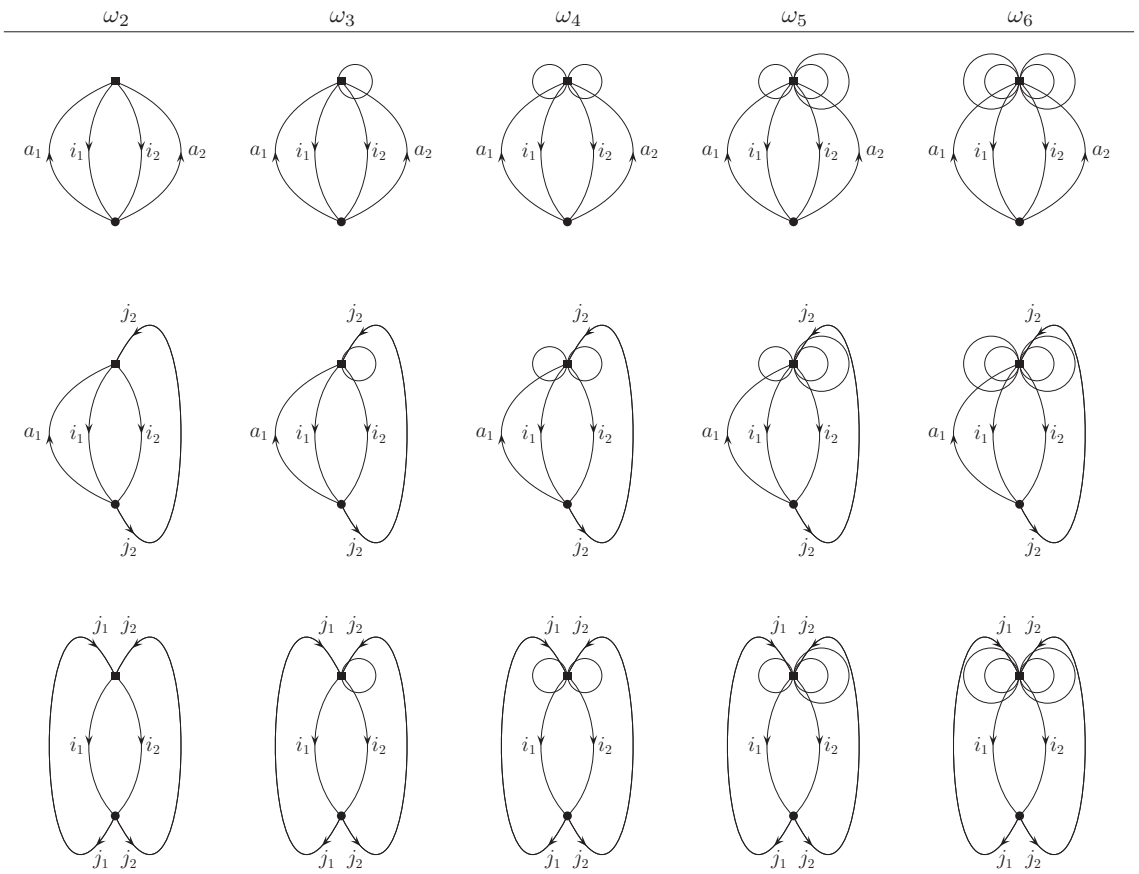

FIG. 2. Diagrams 6–20. From left to right, the w_k operator increases from a two-body operator (w_2) to a six-body operator (w_6). The first row contains diagrams 6 (D_6) through 10 (D_{10}) going across. The second row, diagrams 11 (D_{11}) through 15 (D_{15}). The third row, diagrams 16 (D_{16}) through 20 (D_{20}).

and k_2 represents the occupied states. We note that the strength of the particle-hole excitation operator depends on the value of the amplitude, which is functional of g. In this work we are interested in using g to project out weak excitations. We achieve this by defining the following 1p-1h and 2p-2h operators:

$$T_1^\theta[\eta] = \sum_{ia} \theta_{ia} t_{ia} \{a^\dagger i\}, \tag{13}$$

$$T_2^\theta[\eta] = \sum_{i<j,a<b} \theta_{ijab} t_{ijab} \{a^\dagger b^\dagger j i\}, \tag{14}$$

where θ_{ia} and θ_{ijab} are compact notations for the following Heaviside step functions:

$$\theta_{ia}[\eta, g] \equiv \theta(|g_{ia}| - \eta), \tag{15}$$

$$\theta_{ijab}[\eta, g] \equiv \theta(|g^{\mathrm{A}}_{ijab}| - \eta). \tag{16}$$

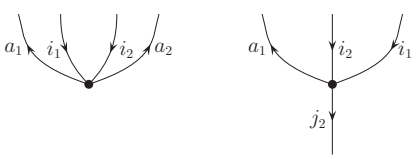

FIG. 3. Left: 2p-2h excitation operator. Right: 1p-1h operator.

In the above equations, we have introduced a control parameter η that projects out particle-hole excitations whose amplitudes are below a certain tolerance value. The one-body and two-body t amplitudes in Eq. (13) and (14) are obtained by applying the geminal-projected particle-hole operators for the construction of the many-electron wave function,

$$\Psi_{\mathrm{exact}} \approx \Omega[T^\theta]\Phi_0, \tag{17}$$

where Ω is a general many-body operator responsible for including electron correlation, and the square bracket denotes that it is a functional of the t amplitudes. In this work, we present three different strategies using configuration interaction, many-body perturbation theory, and coupled-cluster theory for determination of the t amplitudes; and the details of the derivation are presented in Secs. II C 1, II C 2, and II C 3, respectively.

B. Determination of correlation function

In this work, the R12-correlation operator is represented using Gaussian-type geminal functions as shown in the following equation:

$$g(\mathbf{r}_1, \mathbf{r}_2) = \sum_{k=1}^{N_g} b_k e^{-r_{12}^2/d_k}, \tag{18}$$

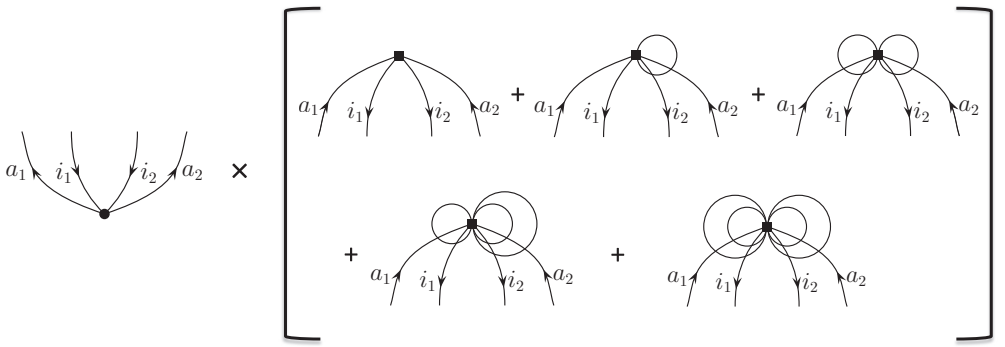

FIG. 4. Factorization of diagrams 6–10 in terms of 2p-2h operator.

where N_g are the number of terms in the expansion and b_k and d_k are expansion parameters. Typically, the expansion parameters are determined using a variational approach by minimizing the energy or its variance. However, such a strategy in not practical in this work because the computational effort for the variational determination of the geminal parameters would be higher than performing the GP-CI calculations. Here, we present an analytical method for determination of the geminal parameters which does not rely on a variational approach.

To keep the analytical derivation tractable we use only one geminal function ($N_g = 1$). The determination of the geminal parameters (b_1,d_1) is based on imposing the the Kato electron-electron cusp condition which is given by the following equation:

$$\left(\frac{\partial \Psi}{\partial r_{12}}\right)_{r_{12}=0} = \frac{1}{2} r_{12}. \tag{19}$$

Unfortunately, Gaussian-type geminal (GTG) functions do not have the necessary analytical properties to satisfy the above condition. The Kato cusp condition in principle, can be realized by using a Slater-type geminal (STG) function,

$$\phi_{\mathrm{STG}}(r_{12}) = e^{-\frac{1}{2} r_{12}}. \tag{20}$$

However, calculation of molecular integrals is more expensive using STG as compared to GTG, and using STG will increase the computational cost and complexity of the overall calculations. Because the GTG function cannot satisfy the exact Kato cusp condition, we imposed the requirements that the geminal parameters must satisfy an approximate condition that is based on the average electron-electron separation distance,

$$\frac{b_1}{d_1} r_{12}^2 \neq \frac{1}{2} r_{12}, \tag{21}$$

$$\frac{b_1}{d_1} \langle r_{12}^2 \rangle = \frac{1}{2} \langle r_{12} \rangle. \tag{22}$$

The motivation for the above condition is based on the previous observations [39,90,91] that the form of the explicitly correlated wave function in the neighborhood of the electron-electron coalescence point plays a significant role in the accurate treatment of electron-electron correlation. Comparing the left and right side of the above equation, we define the geminal parameters as

$$b_1 = \langle r_{12} \rangle, \tag{23}$$

$$d_1 = 2 \langle r_{12}^2 \rangle. \tag{24}$$

The computation of $\langle r_{12} \rangle$ is more expensive than the computation of $\langle r_{12}^2 \rangle$ because the integral over r_{12}^2 using Gaussian-type orbitals (GTOs) can be expressed as sum of x^2, y^2, and z^2 components. Therefore we approximate the average electron-electron distance using the following expression:

$$\langle r_{12} \rangle \approx \sqrt{\langle r_{12}^2 \rangle}. \tag{25}$$

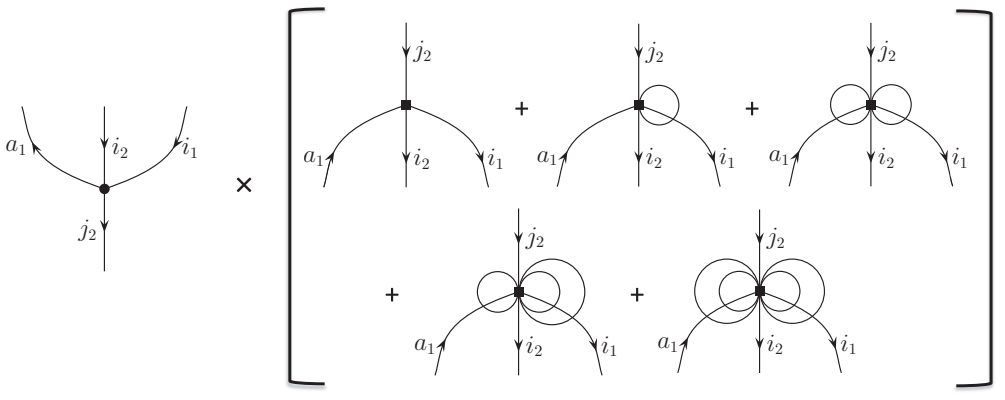

FIG. 5. Factorization of diagrams 11–15 in terms of 1p-1h operator.

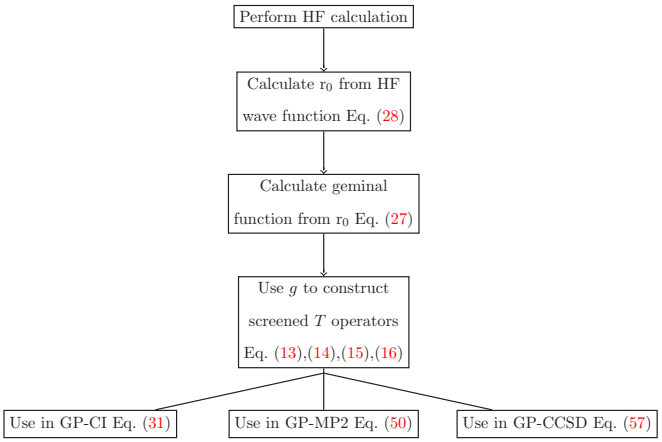

FIG. 6. Flow chart showing the steps involved in GP-CI, GP-MP2, and GP-CCSD theories.

Therefore, we approximate b_1 as

$$b_1 \approx \sqrt{\langle r_{12}^2 \rangle}. \tag{26}$$

Substituting in the values for d_1 from Eq. (24) and b_1 from Eq. (26) into Eq. (18), we arrive at the final expression for the geminal function (in atomic units)

$$g(r_{12}) = \left(\frac{\sqrt{\langle r_{12}^2 \rangle}}{1 \text{ a.u.}} \right) \exp\left[-\frac{r_{12}^2}{2\langle r_{12}^2 \rangle} \right]. \tag{27}$$

The square of the electron-electron separation distance is obtained from the Hartree-Fock wave function using the expression

$$\langle r_{12}^2 \rangle = \frac{2}{N(N-1)} \langle 0| \sum_{i<j} r_{ij}^2 |0\rangle. \tag{28}$$

C. Construction of geminal-projected correlated wave functions

The geminal-projected particle-hole (GPPH) operators (1p-1h and 2p-2h) can be used in various many-body theories for treating electron-electron correlation. The t amplitudes (t_{ia} and t_{ijab}) in the GPPH can be determined using different existing strategies for treating electron-electron correlation. In this work, we present three different proof-of-concept strategies for calculating the t amplitudes using variational, many-body perturbation theory (MBPT), and coupled-cluster theory.

TABLE I. CISD ground-state energy (in Hartrees) of CH_4 calculated using analytical geminal parameters and varying η.

η	$N_{\text{GP-CI}}$	$E_{\text{GP-CI}}$	$N_{\text{CISD}}/N_{\text{GP-CI}}$	$E_{\text{GP-CI}} - E_{\text{CISD}}$
10^{-1}	39	−40.194994	736.18	1.56×10^{-1}
10^{-2}	354	−40.269236	81.10	8.19×10^{-2}
10^{-3}	4336	−40.346046	6.62	5.06×10^{-3}
10^{-4}	8004	−40.351015	3.59	8.71×10^{-5}
10^{-5}	8919	−40.351072	3.22	3.04×10^{-5}
CISD	28711	−40.351102	1.00	0.00

TABLE II. CISD ground-state energy (in Hartrees) of NH_3 calculated using analytical geminal parameters and varying η.

η	$N_{\text{GP-CI}}$	$E_{\text{GP-CI}}$	$N_{\text{CISD}}/N_{\text{GP-CI}}$	$E_{\text{GP-CI}} - E_{\text{CISD}}$
10^{-1}	29	−56.183815	780.72	1.81×10^{-1}
10^{-2}	265	−56.296168	85.44	6.85×10^{-2}
10^{-3}	2214	−56.360953	10.23	3.76×10^{-3}
10^{-4}	3221	−56.364358	7.03	3.50×10^{-4}
10^{-5}	3599	−56.364668	6.29	4.02×10^{-5}
CISD	22641	−56.364708	1.00	0

1. Configuration interaction

To determine the t amplitudes using the variational procedure, we construct the GP-CI operator which is defined as

$$\Omega_{\text{GP-CI}}[\eta, g] = 1 + T_1^{\theta}[\eta, g] + T_2^{\theta}[\eta, g]. \tag{29}$$

The GP-CI wave function is defined as

$$\Psi_{\text{GP-CI}} = \Omega_{\text{GP-CI}} |\Phi_0\rangle. \tag{30}$$

The t amplitudes are obtained variationally by minimizing the total energy

$$E_{\text{GP-CI}}[\eta, g] = \min_{t_{ia}, t_{ijab}} \frac{\langle 0|\Omega_{\text{GP-CI}}^{\dagger} H \Omega_{\text{GP-CI}}|0\rangle}{\langle 0|\Omega_{\text{GP-CI}}^{\dagger} \Omega_{\text{GP-CI}}|0\rangle}. \tag{31}$$

The implementation of the this approach is straightforward and is identical to the conventional CI single and double excitations (CISD) implementation. However, it is important to note that unlike the conventional CISD method, the size of the GP-CI matrix depends on the choice of g and η. The total number of terms in the $\Omega_{\text{GP-CI}}$ is given by,

$$N_{\text{GP-CI}}[\eta, g] = 1 + \sum_{ia} \theta_{ia} + \sum_{i<j, a<b} \theta_{ijab}. \tag{32}$$

In the limit of $\eta \to 0$, the method should reduce to the conventional CISD method,

$$\lim_{\eta \to 0} N_{\text{GP-CI}} = N_{\text{CISD}}, \tag{33}$$

$$\lim_{\eta \to 0} \Omega_{\text{GP-CI}} = \Omega_{\text{CISD}}, \tag{34}$$

$$\lim_{\eta \to 0} E_{\text{GP-CI}} = E_{\text{CISD}}. \tag{35}$$

TABLE III. CISD ground-state energy (in Hartrees) of H_2O calculated using analytical geminal parameters and varying η.

η	$N_{\text{GP-CI}}$	$E_{\text{GP-CI}}$	$N_{\text{CISD}}/N_{\text{GP-CI}}$	$E_{\text{GP-CI}} - E_{\text{CISD}}$
10^{-1}	25	−76.010000	691.64	1.90×10^{-1}
10^{-2}	235	−76.149998	73.58	5.03×10^{-2}
10^{-3}	1192	−76.197151	14.51	3.12×10^{-3}
10^{-4}	1709	−76.199857	10.12	4.15×10^{-4}
10^{-5}	1905	−76.200269	9.08	3.31×10^{-6}
CISD	17291	−76.200272	1.00	0

TABLE IV. CISD ground-state energy (in Hartrees) of HF calculated using analytical geminal parameters and varying η.

η	$N_{\text{GP-CI}}$	$E_{\text{GP-CI}}$	$N_{\text{CISD}}/N_{\text{GP-CI}}$	$E_{\text{GP-CI}} - E_{\text{CISD}}$
10^{-1}	27	-100.002394	468.93	1.80×10^{-1}
10^{-2}	177	-100.136821	71.53	4.56×10^{-2}
10^{-3}	937	-100.179458	13.51	2.96×10^{-3}
10^{-4}	1602	-100.182291	7.90	1.28×10^{-4}
10^{-5}	1919	-100.182410	6.60	8.50×10^{-6}
CISD	12661	-100.182419	1.00	0

TABLE V. CISD ground-state energy (in Hartrees) of Ne calculated using analytical geminal parameters and varying η.

η	$N_{\text{GP-CI}}$	$E_{\text{GP-CI}}$	$N_{\text{CISD}}/N_{\text{GP-CI}}$	$E_{\text{GP-CI}} - E_{\text{CISD}}$
10^{-1}	13	-128.474407	673.15	1.50×10^{-1}
10^{-2}	97	-128.592196	90.22	3.24×10^{-2}
10^{-3}	479	-128.622321	18.27	2.28×10^{-3}
10^{-4}	1013	-128.624309	8.64	2.89×10^{-4}
10^{-5}	1240	-128.624596	7.06	1.53×10^{-6}
CISD	8751	-128.624598	1.00	0

In the limit $\eta \to \infty$, the method reduces to the Hartree-Fock method,

$$\lim_{\eta\to\infty} N_{\text{GP-CI}} = 1, \tag{36}$$

$$\lim_{\eta\to\infty} \Omega_{\text{GP-CI}} = 1, \tag{37}$$

$$\lim_{\eta\to\infty} E_{\text{GP-CI}} = E_{\text{HF}}. \tag{38}$$

2. *Many-body perturbation theory*

The derivation of the time-independent perturbation theory is well known and has been derived in the literature using different theoretical formulations [92–94]. In this work, we use the Rayleigh-Schrödinger perturbation theory (RSPT) approach to illustrate the application of the GPPH operators in perturbation theory. In the RSPT, the ground-state wave function and energy are defined using the following expansion:

$$|\Psi_{\text{RSPT}}\rangle = \Phi_0 + \Psi^{(1)} + \Psi^{(2)} + \cdots, \tag{39}$$

$$E = E^{(0)} + E^{(1)} + E^{(2)} + \cdots, \tag{40}$$

where Φ_0 and $E^{(0)}$ are the unperturbed wave function and ground-state energy, respectively. The expressions for the perturbed wave functions and energies are obtained by first substituting the above expansion in the exact Schrödinger equation and then performing a term-by-term analysis [92–94]

$$(E^{(0)} - H_0)\Psi^{(n)} = W\Psi^{(n-1)} - \sum_{i=0}^{n-1} E^{(n-i)}\Psi^{(i)}, \tag{41}$$

where W is the perturbing potential $W = H - H_0$. Using Eq. (41), the nth-order correction to the exact ground-state energy is given in terms of the perturbing potential W,

$$E^{(n)} = \langle\Phi_0|W|\Psi^{(n-1)}\rangle. \tag{42}$$

The perturbed wave function is expressed in terms of the resolvent operator R_0 which is defined as

$$R_0 = (E_0 - H_0)^{-1}, \tag{43}$$

where H_0 and E_0 are the unperturbed Hamiltonian and unperturbed ground-state energy, respectively. Using Eqs. (41) and (43), the nth-order perturbed wave function can be expressed as

$$|\Psi^{(n)}\rangle = R_0 W|\Psi^{(n-1)}\rangle - \sum_{i=0}^{n-1} E^{(n-i)} R_0|\Psi^{(i)}\rangle. \tag{44}$$

In conventional RSPT, the perturbed wave function is expanded in the basis of the eigenfunctions of the H_0 [92–94]

$$|\Psi^{(n)}\rangle_{\text{RSPT}} = \left[\sum_{ia} t_{ia} a^\dagger i + \sum_{i<j,a<b} t_{ijab} a^\dagger b^\dagger ji + \sum_{i<j<k,a<b<c} t_{ijkabc} a^\dagger b^\dagger c^\dagger kji + \ldots\right]|\Phi_0\rangle, \tag{45}$$

where the amplitudes (t_{ia},t_{ijab}, . . .) are obtained by substituting Eq. (45) in Eq. (44). In the geminal-projected RSPT (GP-RSPT) method, we use the projected particle-hole operators defined in Eq. (14) to construct the perturbed wave function,

$$|\Psi^{(n)}\rangle_{\text{GP-RSPT}} = \left[\sum_{ia} t_{ia}\theta_{ia} a^\dagger i + \sum_{i<j,a<b} t_{ijab}\theta_{ijab} a^\dagger b^\dagger ji + \sum_{i<j<k,a<b<c} t_{ijkabc} a^\dagger b^\dagger c^\dagger kji + \cdots\right]|\Phi_0\rangle. \tag{46}$$

We note that because the GPPH operators span only 1p-1h and 2p-2h excitation space; 3p-3h and higher-order operators in the above expression are identical to the RSPT equation

$$|\Psi^{(n)}\rangle_{\text{GP-RSPT}} = \left[T_1^\theta + T_2^\theta + \sum_{i<j<k,a<b<c} t_{ijkabc} a^\dagger b^\dagger c^\dagger kji + \cdots\right]|\Phi_0\rangle. \tag{47}$$

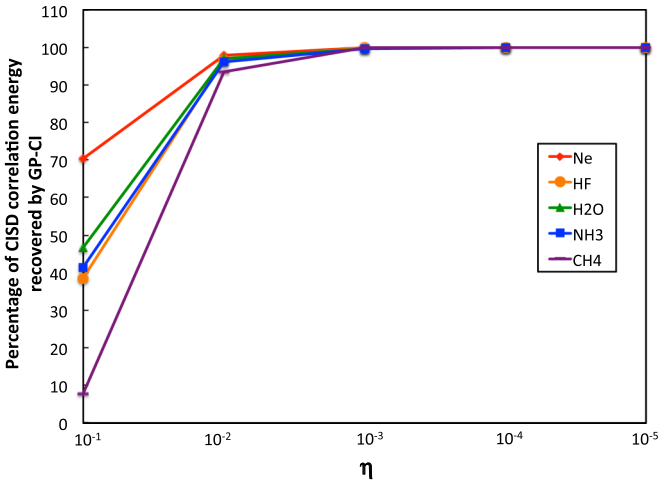

FIG. 7. Analysis of the percentage of CISD correlated energy recovered by the GP-CI method as a function of the tolerance parameter η.

In this work, we have used the the Møller-Plesset (MP) partitioning of the many-electron Hamiltonian where the zeroth-order Hamiltonian H_0 is the Fock operator and the perturbing potential is the difference between the electron-electron Coulomb operator $V_{\rm ee}$ and the Hartree-Fock potential

$$W = V_{\rm ee} - \langle\Phi_0|V_{\rm ee}|\Phi_0\rangle. \tag{48}$$

The second-order Møller-Plesset energy is given by the expression [92,93]

$$E^{(2)}_{\rm MP2} = \frac{1}{4}\sum_{ijab}\frac{|\langle ij|r_{12}^{-1}|ab\rangle_A|^2}{(\epsilon_i+\epsilon_j-\epsilon_a-\epsilon_b)}. \tag{49}$$

Using Eq. (47), the analogous equation for the geminal-project Møller-Plesset (GP-MP) perturbation theory is given by the following expression:

$$E^{(2)}_{\rm GP-MP2}[\eta,g] = \frac{1}{4}\sum_{ijab}\theta_{ijab}\frac{|\langle ij|r_{12}^{-1}|ab\rangle_A|^2}{(\epsilon_i+\epsilon_j-\epsilon_a-\epsilon_b)}. \tag{50}$$

The number of terms in the above expression depend on the choice of η and g and is given by

$$N_{\rm GP-MP2}[\eta,g] = \frac{1}{4}\sum_{ijab}\theta_{ijab}. \tag{51}$$

TABLE VI. MP2 ground-state energy (in Hartrees) of CH_4 calculated using analytical geminal parameters and varying η.

η	$N_{\rm GP\text{-}MP2}$	$E_{\rm GP\text{-}MP2}$	$N_{\rm MP2}/N_{\rm GP\text{-}MP2}$	$E_{\rm GP\text{-}MP2}-E_{\rm MP2}$
10^{-1}	1	−40.194994	28351	1.42×10^{-1}
10^{-2}	268	−40.229412	105.79	1.08×10^{-1}
10^{-3}	4248	−40.312698	6.67	2.43×10^{-2}
10^{-4}	7916	−40.334316	3.58	2.72×10^{-3}
10^{-5}	8831	−40.336758	3.21	2.74×10^{-4}
MP2	28351	−40.337032	1.00	0.00

TABLE VII. MP2 ground-state energy (in Hartrees) of NH_3 calculated using analytical geminal parameters and varying η.

η	$N_{\rm GP\text{-}MP2}$	$E_{\rm GP\text{-}MP2}$	$N_{\rm MP2}/N_{\rm GP\text{-}MP2}$	$E_{\rm GP\text{-}MP2}-E_{\rm MP2}$
10^{-1}	1	−56.183815	22321	1.74×10^{-1}
10^{-2}	215	−56.291308	103.82	6.61×10^{-2}
10^{-3}	2156	−56.354307	10.35	3.07×10^{-3}
10^{-4}	3159	−56.357209	7.07	1.67×10^{-4}
10^{-5}	3523	−56.357356	6.34	2.06×10^{-5}
MP2	22321	−56.357376	1.00	0

3. *Coupled-cluster theory*

The GPPH operators can also be used in coupled-cluster theory. In this work, we present formulation for the geminal-projected analogs of CCSD theory, which is defined by the following expression:

$$|\Psi\rangle_{\rm GP-CCSD} = e^{T_1^\theta+T_2^\theta}|\Phi_0\rangle. \tag{52}$$

The coupled-cluster equation in terms of the normal-ordered Hamiltonian H_N is given as

$$H_N e^{T_1^\theta+T_2^\theta}|\Phi_0\rangle = \Delta E e^{T_1^\theta+T_2^\theta}|\Phi_0\rangle, \tag{53}$$

where ΔE is the correlation energy and $H_N = H - \langle\Phi_0|H|\Phi_0\rangle$. Performing similarity transformation gives us the equations for correlation energy and t amplitudes:

$$\langle\Phi_0|e^{-T_1^\theta+T_2^\theta}H_N e^{T_1^\theta+T_2^\theta}|\Phi_0\rangle_C = \Delta E, \tag{54}$$

$$\langle\Phi_i^a|e^{-T_1^\theta+T_2^\theta}H_N e^{T_1^\theta+T_2^\theta}|\Phi_0\rangle_C = 0, \tag{55}$$

$$\langle\Phi_{ij}^{ab}|e^{-T_1^\theta+T_2^\theta}H_N e^{T_1^\theta+T_2^\theta}|\Phi_0\rangle_C = 0, \tag{56}$$

where the subscript C implies that only connected terms are included in evaluating the expressions [93–95]. The equations for the t amplitudes are obtained by performing the Baker-Campbell-Hausdorff expansion of the similarity-transformed Hamiltonian and are well-documented in the literature [93–95]. The t-amplitude equations are solved iteratively, the total correlation energy is calculated from them using the expression [93–95]

$$\Delta E_{\rm GP-CCSD}[\eta,g] = \frac{1}{4}\sum_{ijab}t_{ijab}\theta_{ijab}\langle ij|r_{12}^{-1}|ab\rangle_A + \frac{1}{2}\sum_{ijab}t_{ia}t_{jb}\theta_{ia}\theta_{jb}\langle ij|r_{12}^{-1}|ab\rangle_A. \tag{57}$$

TABLE VIII. MP2 ground-state energy (in Hartrees) of H_2 O calculated using analytical geminal parameters and varying η.

η	$N_{\rm GP\text{-}MP2}$	$E_{\rm GP\text{-}MP2}$	$N_{\rm MP2}/N_{\rm GP\text{-}MP2}$	$E_{\rm GP\text{-}MP2}-E_{\rm MP2}$
10^{-1}	1	−76.010000	17011	1.89×10^{-1}
10^{-2}	193	−76.148962	88.14	5.03×10^{-2}
10^{-3}	1140	−76.196804	14.92	2.43×10^{-3}
10^{-4}	1655	−76.198907	10.28	3.27×10^{-4}
10^{-5}	1851	−76.199232	9.19	2.08×10^{-6}
MP2	17011	−76.199234	1.00	0

TABLE IX. MP2 ground-state energy (in Hartrees) of HF calculated using analytical geminal parameters and varying η.

η	$N_{\text{GP-MP2}}$	$E_{\text{GP-MP2}}$	$N_{\text{MP2}}/N_{\text{GP-MP2}}$	$E_{\text{GP-MP2}} - E_{\text{MP2}}$
10^{-1}	1	−100.002394	12421	1.82×10^{-1}
10^{-2}	139	−100.136290	89.36	4.79×10^{-2}
10^{-3}	889	−100.179077	13.97	5.08×10^{-3}
10^{-4}	1550	−100.183800	8.01	3.57×10^{-4}
10^{-5}	1867	−100.184153	6.65	3.92×10^{-6}
MP2	12421	−100.184157	1.00	0

This expression is similar to the conventional CCSD energy expression; however, the number of terms in Eq. (57) depends on η and g, which can be calculated using the procedure described earlier for GP-CI method.

III. RESULTS AND DISCUSSION

The effectiveness of the GPPH method was analyzed by performing proof-of-concept calculations on representative many-electron systems. We implemented both GP-CI and GP-MP2 methods and steps involved in the calculations are summarized in Fig. 6. As seen in Fig. 6, the first four steps involved construction of the GPPH operators, and the final step involved construction of the CI and first-order wave functions for GP-CI and GP-MP2 methods, respectively. The GP-CI method was tested on a set of isoelectronic 10-electron systems: CH_4, NH_3, H_2O, HF, and Ne; and the calculated ground-state energies were compared with CISD results. In all cases, the calculations were performed using 6-31 $G^\star$ basis functions. We defined two important metrics for analyzing the GP-CI results. The first is the difference between CISD and GP-CI energies E_{diff} and the second is the ratio of the number of variational parameters between the two methods [Eqs. (58) and (59)]:

$$E_{\text{diff}}(\eta) = E_{\text{GP-CI}}(\eta) - E_{\text{CISD}}, \tag{58}$$

$$R(\eta) = \frac{N_{\text{CISD}}}{N_{\text{GP-CI}}(\eta)}. \tag{59}$$

As presented in Eq. (32), the number of variational parameters in the GP-CI method depends on the choice of the η and for these calculations η was varied from 10^{-1} to 10^{-5}. In Tables I–V we observe a significant reduction in the size of the CI space, while not sacrificing accuracy in the calculated ground-state energy. Using the GP-CI method on the systems studied, the CI space was reduced by a factor of 6 while still maintaining ground-state energies with accuracy of 10^{-6} Hartrees with respect to the CISD energy. For example, in case of neon, the GP-CI method was able to give an accuracy of 10^{-3} Hartrees as compared to CISD results while using a configuration space that is 19 times smaller than the CISD calculation. The accuracy of the GP-CI method can be systematically increased by decreasing the η parameter and for the neon atom, 10^{-6} Hartrees accuracy was achieved by using a configuration space that was 7 times smaller than the CISD calculation. The percentage of CISD correlation energy recovered by the GP-CI method as a function of the cutoff parameter η is presented in Fig. 7. In all cases, we found that more than 90% of CISD correlation energy was recovered when η is in the range of 10^{-2}–10^{-3}. The results from GP-MP2 were also found to follow a similar trend and are presented in Tables VI–X. The results from both GP-CI and GP-MP2 calculations show the effectiveness of geminal-projected particle-hole operators for construction of many-electron correlated wave functions.

The method presented here is restricted to only the two-body operator G. As a consequence of this choice, only 1p-1h and 2p-2h particle-hole operators can be projected out. In principle, this strategy can be systematically extended to 3p-3h and higher-order operators by including three-body and higher terms in the correlation function G. However, it is important to note that the use of geminal-projected particle-hole operators is intrinsically approximate because it projects out noncontributing terms and therefore cannot be used for construction of the exact many-electron wave function. However, the strength of the geminal-projected particle-hole operators lies in numerically efficient implementation of approximate many-electron theories such as configuration interaction, many-body perturbation theory, and coupled-cluster theory.

The method can also be combined with other theories that include explicit treatment of electron-electron cusp in the many-electron wave function. For example, the geminal-projected particle-hole operators can be used in multideterminant quantum Monte Carlo and F12 methods including MP2-F12 and CCSD-F12 methods. In addition to the electron-electron cusp condition, a systematic improvement of the electron-nuclear cusp condition can be achieved by using Slater-type orbitals and electron-nuclear Jastrow functions.

TABLE X. MP2 ground-state energy (in Hartrees) of Ne calculated using analytical geminal parameters and varying η.

η	$N_{\text{GP-MP2}}$	$E_{\text{GP-MP2}}$	$N_{\text{MP2}}/N_{\text{GP-MP2}}$	$E_{\text{GP-MP2}} - E_{\text{MP2}}$
10^{-1}	1	−128.474407	8551	1.52×10^{-1}
10^{-2}	75	−128.523031	114.01	1.03×10^{-1}
10^{-3}	453	−128.547410	18.88	7.88×10^{-2}
10^{-4}	987	−128.616193	8.66	9.98×10^{-3}
10^{-5}	1214	−128.625523	7.04	6.53×10^{-4}
MP2	8551	−128.626176	1.00	0

FIG. 8. Diagram showing a particle and hole for the Slater determinant Φ_i^a.

FIG. 9. Diagram showing particles and holes for the Slater determinant Φ_{ij}^{ab}.

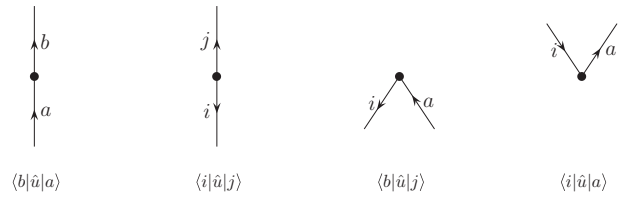

FIG. 10. One-particle operators in diagrammatic representation.

IV. CONCLUSIONS

The derivation of the geminal-projected particle-hole excitation operators was presented. The central idea underlying this method is the use of an explicitly correlated reference wave function to define a projecting operator that projects out potential noncontributing configurations in the CI expansion. In this work, the explicitly correlated reference function was defined using a two-body Gaussian-type geminal function. The derivation of the projection operator was performed by first expressing the total energy in terms of Hugenholtz diagrams and then factorizing out particle-hole excitation operators that are functionals of the R12-correlator operator. The efficiency of the projection operation is controlled by a tunable external parameter. The projected particle-hole operators were used for the construction of the geminal-projected CI wave function which was subsequently used to perform proof-of-concept ground-state energy calculations on a set of molecules. The results from these calculations demonstrate that the method shows much promise since in all cases the geminal-projected CI wave function was found to deliver CISD-level accuracy using a CI space that is at least six times smaller than the CISD space. The results from this work highlight the efficacy of the geminal-projected particle-hole operators for reducing the number of optimizable parameters in a correlated many-electron wave function. The application of geminal-projected particle-hole operators derived in this work is not restricted to a CI wave function and was demonstrated to be applicable to many-body perturbation theory and coupled-cluster theory

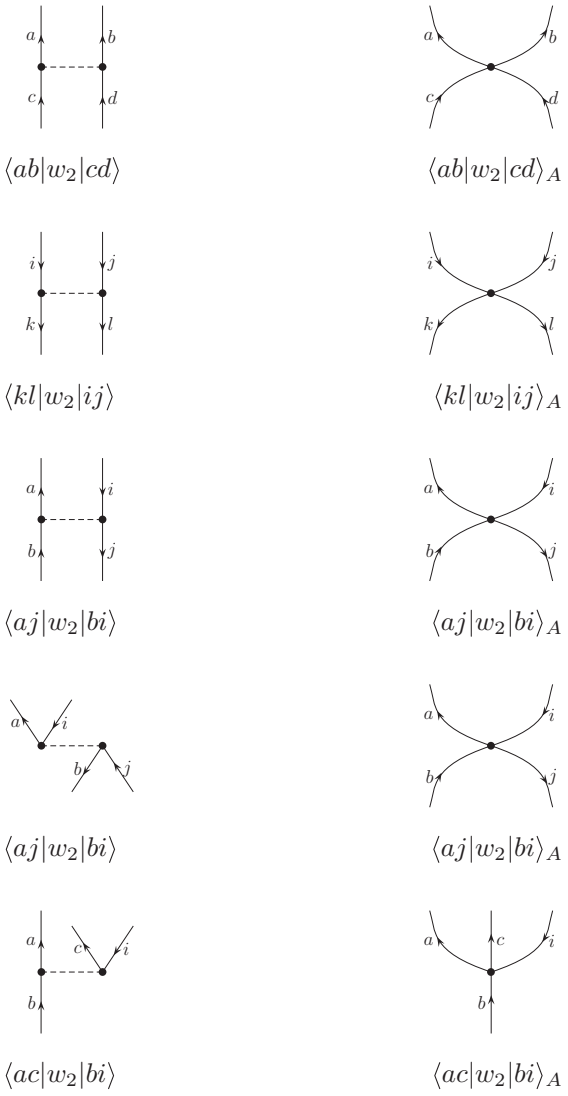

FIG. 11. Two-body Goldstone diagrams (left); two-body Hugenholtz diagrams (right). Part 1.

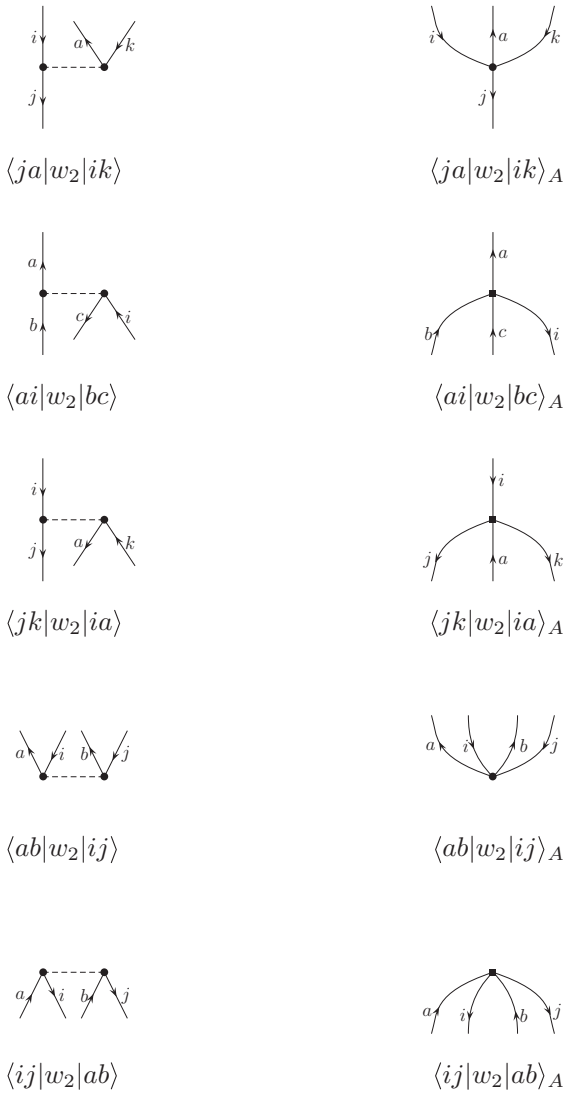

FIG. 12. Same as Fig. 11, but Part 2. .

as well. We envision that geminal-projected particle-hole excitation operators can also be used in multideterminant quantum Monte Carlo methods.

ACKNOWLEDGMENTS

Acknowledgment is made to Syracuse University, NSF REU Grant No. CHE-1263154, and the donors of the American Chemical Society Petroleum Research Fund for support under Grant No. 52659-DNI6 of this research.

APPENDIX

In this Appendix, we briefly summarize the Goldstone and Hugenholtz diagrammatic representations which were used in the derivation of the geminal-projected particle-hole operators. The one-particle operators for both the Goldstone and Hugenholtz representations have the same form, but the two-particle operators have slightly different form for each representation. We start by considering the singly excited Slater determinant, $\Phi_i^a = \{a^\dagger i\}\Phi_0$, before we consider the one-particle operators. Here we follow the convention of labeling the occupied and unoccupied states by indices i,j,k,l and a,b,c,d, respectively. The occupied indices are used to refer to the hole states and the unoccupied indices are used to refer to the particle states [93]. This Slater determinant is represented diagrammatically with a particle line pointing upward and a hole line pointing downward as seen in Fig. 8. Similarly, the doubly excited Slater determinant $\Phi_{ij}^{ab} = \{a^\dagger b^\dagger ji\}\Phi_0$, the diagrammatic representation has two particle lines, a and b, and two hole lines, i and j, as seen in Fig. 9. Now we consider diagrammatic notation for the one-particle operator $\hat{u}$. The form of the one-particle operator can be written as $\langle p|\hat{u}|q\rangle$ where p and q can be particle or hole lines. There are four possibilities for representing the one-particle operator. It can be particle-particle, hole-hole, particle-hole, or hole-particle, where we will use a and b as particle states and i and j as hole states. These four cases are seen in Fig. 10. The bold dot in the diagrams represents the operator $\hat{u}$ and it occurs at the vertex of two lines. Each vertex needs one incoming line and one outgoing line. In relation to the operator dot, the incoming line is the ket state, while the outgoing line is the bra state. The two-particle operators are consistent with this notation used by the one-particle operators.

For the two-particle operators in the Goldstone representation, there is no longer one vertex. The one vertex is split into two half-vertices which are connected by a dashed interaction line. The two half-vertices and the interaction line constitute a single vertex. In the Hugenholtz representation, the diagrams are compacted so that there is only one vertex in each two-body diagram. The relationship between the Goldstone and Hugenholtz diagrams and the corresponding matrix elements are shown in Figs. 11 and 12.

[1] C. D. Sherrill and H. F. Schaefer, III Adv. Quantum Chem. **34**, 143 (1999).
[2] C. F. Bender and E. R. Davidson, Phys. Rev. **183**, 23 (1969).
[3] B. Huron, J. P. Malrieu, and P. Rancurel, J. Chem. Phys. **58**, 5745 (1973).
[4] R. Buenker and S. Peyerimhoff, Theor. Chim. Acta **35**, 33 (1974).
[5] S. Evangelisti, J.-P. Daudey, and J.-P. Malrieu, Chem. Phys. **75**, 91 (1983).
[6] D. Feller and E. R. Davidson, J. Chem. Phys. **90**, 1024 (1989).
[7] R. J. Harrison, J. Chem. Phys. **94**, 5021 (1991).
[8] R. Roth and P. Navrátil, Phys. Rev. Lett. **99**, 092501 (2007).
[9] R. Roth, Phys. Rev. C **79**, 064324 (2009).
[10] Z. Gershgorn and I. Shavitt, Int. J. Quantum Chem. **2**, 751 (1968).
[11] J. Ivanic and K. Ruedenberg, Theor. Chem. Acc. **106**, 339 (2001).
[12] J. Ivanic and K. Ruedenberg, Theor. Chem. Acc. **107**, 220 (2002).
[13] A. L. Wulfov, Chem. Phys. Lett. **255**, 300 (1996).
[14] P. J. Bruna, S. D. Peyerimhoff, and R. J. Buenker, Chem. Phys. Lett. **72**, 278 (1980).
[15] S. Saebø, J. Almlöf, J. E. Boggs, and J. G. Stark, J. Mol. Struct.: THEOCHEM **200**, 361 (1989).
[16] P. Pulay, Chem. Phys. Lett. **100**, 151 (1983).
[17] P. Pulay and S. Saebø, Theor. Chim. Acta **69**, 357 (1986).
[18] S. Saebø and P. Pulay, J. Chem. Phys. **86**, 914 (1987).
[19] C. Hampel and H. Werner, J. Chem. Phys. **104**, 6286 (1996).
[20] G. Hetzer, P. Pulay, and H.-J. Werner, Chem. Phys. Lett. **290**, 143 (1998).
[21] M. Schütz, G. Hetzer, and H.-J. Werner, J. Chem. Phys. **111**, 5691 (1999).
[22] T. S. Chwee, A. B. Szilva, R. Lindh, and E. A. Carter, J. Chem. Phys. **128**, 224106 (2008).
[23] T. S. Chwee and E. A. Carter, J. Chem. Phys. **132**, 074104 (2010).
[24] T. S. Chwee and E. A. Carter, Mol. Phys. **108**, 2519 (2010). .
[25] J. C. Greer, J. Chem. Phys. **103**, 7996 (1995).
[26] J. C. Greer, J. Chem. Phys. **103**, 1821 (1995).
[27] J. Greer, J. Comput. Phys. **146**, 181 (1998).
[28] G. H. Booth, A. J. W. Thom, and A. Alavi, J. Chem. Phys. **131**, 054106 (2009).
[29] D. Cleland, G. H. Booth, and A. Alavi, J. Chem. Phys. **132**, 041103 (2010).
[30] D. Cleland, G. H. Booth, C. Overy, and A. Alavi, J. Chem. Theor. Comput. **8**, 4138 (2012).
[31] M. Sambataro, D. Gambacurta, and L. Lo Monaco, Phys. Rev. B **83**, 045102 (2011).
[32] N. S. Blunt, S. D. Smart, J. A. F. Kersten, J. S. Spencer, G. H. Booth, and A. Alavi, J. Chem. Phys. **142**, 184107 (2015).
[33] F. R. Petruzielo, A. A. Holmes, H. J. Changlani, M. P. Nightingale, and C. J. Umrigar, Phys. Rev. Lett. **109**, 230201 (2012).
[34] L. Bytautas, T. M. Henderson, C. A. Jiménez-Hoyos, J. K. Ellis, and G. E. Scuseria, J. Chem. Phys. **135**, 044119 (2011).
[35] P. Löwdin, J. Math. Phys. **3**, 969 (1962).
[36] P.-O. Löwdin, Phys. Rev. **139**, A357 (1965).
[37] P. Löwdin, J. Chem. Phys. **43**, S175 (1965).
[38] S. Ten-no, J. Chem. Phys. **138**, 164126 (2013).

[39] L. Kong, F. A. Bischoff, and E. F. Valeev, Chem. Rev. **112**, 75 (2012).

[40] W. A. Lester, B. Hammond, and P. Reynolds, *Monte Carlo Methods in Ab Initio Quantum Chemistry* (World Scientific, Singapore, 1994).

[41] M. P. Nightingale and C. J. Umrigar, *Quantum Monte Carlo Methods in Physics and Chemistry* (Springer, Berlin, 1998), Vol. 525.

[42] B. Braïda, J. Toulouse, M. Caffarel, and C. J. Umrigar, J. Chem. Phys. **134**, 084108 (2011).

[43] F. R. Petruzielo, J. Toulouse, and C. J. Umrigar, J. Chem. Phys. **136**, 124116 (2012).

[44] C. Filippi and S. Fahy, J. Chem. Phys. **112**, 3523 (2000).

[45] J. Xu and K. D. Jordan, J. Phys. Chem. A **114**, 1364 (2010).

[46] J. Xu, M. J. Deible, K. A. Peterson, and K. D. Jordan, J. Chem. Theor. Comput. **9**, 2170 (2013).

[47] F.-F. Wang, M. J. Deible, and K. D. Jordan, J. Phys. Chem. A **117**, 7606 (2013).

[48] M. J. Deible, M. Kessler, K. E. Gasperich, and K. D. Jordan, J. Chem. Phys. **143**, 084116 (2015).

[49] M. Deible and K. Jordan, Chem. Phys. Lett. **644**, 117 (2016).

[50] S. Boys and N. Handy, Proc. R. Soc. London A **310**, 43 (1969).

[51] C. J. Umrigar, K. G. Wilson, and J. W. Wilkins, Phys. Rev. Lett. **60**, 1719 (1988).

[52] C. Filippi and C. Umrigar, J. Chem. Phys. **105**, 213 (1996).

[53] S. Lee, L. Jönsson, J. W. Wilkins, G. W. Bryant, and G. Klimeck, Phys. Rev. B **63**, 195318 (2001).

[54] F. Schautz, F. Buda, and C. Filippi, J. Chem. Phys. **121**, 5836 (2004).

[55] F. Schautz and C. Filippi, J. Chem. Phys. **120**, 10931 (2004).

[56] A. Scemama and C. Filippi, Phys. Rev. B **73**, 241101 (2006).

[57] J. Toulouse and C. J. Umrigar, J. Chem. Phys. **126**, 084102 (2007).

[58] E. Neuscamman, C. Umrigar, and G.-L. Chan, Phys. Rev. B **85**, 045103 (2012).

[59] R. Guareschi and C. Filippi, J. Chem. Theor. Comput. **9**, 5513 (2013).

[60] C. Daday, C. Knig, O. Valsson, J. Neugebauer, and C. Filippi, J. Chem. Theor. Comput. **9**, 2355 (2013).

[61] S. Moroni, S. Saccani, and C. Filippi, J. Chem. Theor. Comput. **10**, 4823 (2014).

[62] R. C. Clay III and M. A. Morales, J. Chem. Phys. **142**, 234103 (2015).

[63] H. Zulfikri, C. Amovilli, and C. Filippi, J. Chem. Theor. Comput. **12**, 1157 (2016).

[64] J. Elward, J. Hoffman, and A. Chakraborty, Chem. Phys. Lett. **535**, 182 (2012).

[65] C. J. Blanton, C. Brenon, and A. Chakraborty, J. Chem. Phys. **138**, 054114 (2013).

[66] S. Ten-No, Chem. Phys. Lett. **330**, 169 (2000).

[67] T. Yanai and T. Shiozaki, J. Chem. Phys. **136**, 084107 (2012).

[68] F. Manby and P. Knowles, Chem. Phys. Lett. **310**, 561 (1999).

[69] F. R. Manby, H.-J. Werner, T. B. Adler, and A. J. May, J. Chem. Phys. **124**, 094103 (2006).

[70] E. F. Valeev, J. Chem. Phys. **125**, 244106 (2006).

[71] T. Shiozaki and S. Hirata, J. Chem. Phys. **132**, 151101 (2010).

[72] T. Shiozaki, E. F. Valeev, and S. Hirata, J. Chem. Phys. **131**, 044118 (2009).

[73] E. F. Valeev and T. Daniel Crawford, J. Chem. Phys. **128**, 244113 (2008).

[74] A. Köhn and D. P. Tew, J. Chem. Phys. **133**, 174117 (2010).

[75] C. Hättig, D. P. Tew, and A. Köhn, J. Chem. Phys. **132**, 231102 (2010).

[76] A. Köhn, J. Chem. Phys. **130**, 131101 (2009).

[77] T. Shiozaki, M. Kamiya, S. Hirata, and E. F. Valeev, J. Chem. Phys. **130**, 054101 (2009).

[78] S. A. Varganov and T. J. Martínez, J. Chem. Phys. **132**, 054103 (2010).

[79] J. Mitroy, S. Bubin, W. Horiuchi, Y. Suzuki, L. Adamowicz, W. Cencek, K. Szalewicz, J. Komasa, D. Blume, and K. Varga, Rev. Mod. Phys. **85**, 693 (2013).

[80] S. Bubin, M. Pavanello, W.-C. Tung, K. Sharkey, and L. Adamowicz, Chem. Rev. **113**, 36 (2013).

[81] S. Bubin, M. Formanek, and L. Adamowicz, Chem. Phys. Lett. **647**, 122 (2016).

[82] B. Nichols and V. A. Rassolov, J. Chem. Phys. **139**, 104111 (2013).

[83] V. A. Rassolov, J. Chem. Phys. **117**, 5978 (2002).

[84] V. A. Rassolov, F. Xu, and S. Garashchuk, J. Chem. Phys. **120**, 10385 (2004).

[85] V. A. Rassolov and F. Xu, J. Chem. Phys. **126**, 234112 (2007).

[86] V. A. Rassolov and F. Xu, J. Chem. Phys. **127**, 044104 (2007).

[87] B. A. Cagg and V. A. Rassolov, J. Chem. Phys. **141**, 164112 (2014).

[88] P. Jeszenszki, V. Rassolov, P. R. Surján, and Á. Szabados, Mol. Phys. **113**, 249 (2015).

[89] J. M. Elward, J. Hoja, and A. Chakraborty, Phys. Rev. A **86**, 062504 (2012).

[90] M. G. Bayne, J. Drogo, and A. Chakraborty, Phys. Rev. A **89**, 032515 (2014).

[91] D. Prendergast, M. Nolan, C. Filippi, S. Fahy, and J. C. Greer, J. Chem. Phys. **115**, 1626 (2001).

[92] A. Szabo and N. Ostlund, *Modern Quantum Chemistry: Introduction to Advanced Electronic Structure Theory*, Dover Books on Chemistry (Dover, New York, 1989).

[93] I. Shavitt and R. Bartlett, *Many-Body Methods in Chemistry and Physics: MBPT and Coupled-Cluster Theory*, Cambridge Molecular Science (Cambridge University, Cambridge, England, 2009).

[94] P. Jørgensen and J. Simons, *Second Quantization-based Methods in Quantum Chemistry* (Academic, New York, 1981).

[95] R. J. Bartlett and M. Musiał, Rev. Mod. Phys. **79**, 291 (2007).